

Fram Strait sea ice thickness and summer export

T. Krumpen et al.

This discussion paper is/has been under review for the journal The Cryosphere (TC).
Please refer to the corresponding final paper in TC if available.

Recent summer sea ice thickness surveys in the Fram Strait and associated volume fluxes

T. Krumpen¹, R. Gerdes¹, C. Haas², S. Hendricks¹, A. Herber¹, V. Selyuzhenok¹, L. Smedsrud³, and G. Spreen⁴

¹Alfred Wegener Institute, Busse Str. 24, 27570 Bremerhaven, Germany

²York University, Earth & Space Science & Engineering, Petrie 105, 4700 Keele St, Toronto, ON M3J 1P3, Canada

³Geophysical Institute, University Bergen, Allegt. 70, 5020 Bergen, Norway

⁴Norwegian Polar Institute, Fram Centre, Postbox 6606 Langnes, 9296 Tromsø, Norway

Received: 6 August 2015 – Accepted: 7 September 2015 – Published: 30 September 2015

Correspondence to: T. Krumpen (thomas.krumpen@awi.de)

Published by Copernicus Publications on behalf of the European Geosciences Union.

Title Page

Abstract

Introduction

Conclusions

References

Tables

Figures



Back

Close

Full Screen / Esc

Printer-friendly Version

Interactive Discussion



Abstract

Fram Strait is the main gateway for sea ice export out of the Arctic Ocean, and therefore observations there give insight into composition and properties of Arctic sea ice in general and how it varies over time. An extensive data set of ground-based and airborne electromagnetic ice thickness measurements collected between 2001 and 2012 is presented here, including long transects well into the southern part of the Transpolar Drift obtained using fixed-wing aircrafts. The source area for the surveyed ice is primarily the Laptev Sea, and the estimated age is consistent with a decreased from 3 to 2 years between 1990 and 2012. The data consistently also show a general thinning for the last decade, with a decrease in modal thickness of second year and multiyear ice, and a decrease in mean thickness and fraction of ice thicker than 3 m. Local melting in the strait was investigated in two surveys performed in the downstream direction, showing a decrease of $0.19 \text{ m degree}^{-1}$ latitude south of 81° N probably driven by bottom melting from warm water of Atlantic origin. Further north variability in ice thickness is more related to differences in age and deformation. The thickness observations were combined with ice area export estimates to calculate summer volume fluxes of sea ice. This shows that it is possible to determine volume fluxes through Fram Strait during summer when satellite based sea ice thickness information is missing. While the ice area export based on satellite remote sensing shows positive trends since 2001, the mean fluxes during summer (July and August) are small (18 km^3), and long-term trends are uncertain due to the limited surveys available.

1 Introduction

Arctic sea ice extent and thickness have undergone dramatic changes in the past decades: Summer sea ice extent has declined at an annual rate of approximately $12.7 \text{ \% decade}^{-1}$ over the satellite record (Meier et al., 2014; Comiso and Hall, 2014, 1978–present) and its mean thickness has decreased by $0.58 \pm 0.07 \text{ m decade}^{-1}$ over

TCD

9, 5171–5202, 2015

Fram Strait sea ice thickness and summer export

T. Krumpen et al.

Title Page

Abstract

Introduction

Conclusions

References

Tables

Figures

◀

▶

◀

▶

Back

Close

Full Screen / Esc

Printer-friendly Version

Interactive Discussion



Fram Strait sea ice thickness and summer export

T. Krumpfen et al.

Title Page

Abstract

Introduction

Conclusions

References

Tables

Figures



Back

Close

Full Screen / Esc

Printer-friendly Version

Interactive Discussion



the period 2000–2012 (Lindsay and Schweiger, 2015). The thinning of sea ice is accompanied by an increase of ice drift velocity (Spren et al., 2011), deformation (Rampal et al., 2009; Martin et al., 2014) and a decrease of net ice growth rates. Climate model simulations indicate that ice extent and thickness will further decline through the 21st century in response to atmospheric greenhouse gas increases (Vavrus et al., 2012). The mass balance of Arctic sea ice is therefore determined not only by changes in the energy balance of the coupled ice–ocean–atmosphere system but also by the increasing influence of dynamic effects. One aspect of the mass balance of Arctic sea ice are changes of ice volume export rates through Fram Strait, the major sea ice outflow gate of the Arctic.

Trends in southern Fram Strait sea ice thickness were previously investigated by Hansen et al. (2013) and Renner et al. (2014). Based on a 21 year long time series (1990–2011) obtained from moored sonars, Hansen et al. (2013) showed that the ice thickness at 79° N decreased from an annual mean of 3.0 m during the 1990s to 2.2 m during 2008–2011. Renner et al. (2014) reported an even more pronounced thinning of Fram Strait ice cover. According to in-situ and airborne observations carried out at the end of the melt season, ice thickness decreased by over 50 % during 2003–2012. The first aim of this manuscript is to complement those recent findings by means of an extensive data set of electromagnetic (EM) ice thickness observations carried out during summer in northern Fram Strait and the southern part of the Nansen Basin. Measurements were obtained in the months of July and August of 2001, 2004 and 2010–2012 during two cruises of the German ice-breaker RV *Polarstern* and three airborne campaigns with the German DC3-T research aircraft *Polar-5*. An investigation of back trajectories of surveyed sea ice using satellite based sea ice motion data will allow us to examine the connection between thickness variability, ice age and source area.

A second objective of this paper is to investigate across- and along-Fram Strait gradients in sea ice thickness. According to ULS observations of Hansen et al. (2013), the ice thickness distribution in Fram Strait is characterized by a gradient from thicker

timates shall improve the understanding of interannual variability in summer sea ice outflow and complement existing winter volume flux calculations.

2 Data

2.1 EM ice thickness measurements

5 EM ice thickness measurements utilize the contrast of electrical conductivity between sea water and sea ice to determine the distance of the instrument to the ice–water interface (Haas et al., 2009). In 2001 during the RV *Polarstern* cruise (ARK-XVII/2), only ground-based EM (GEM) data were obtained using an instrument (Geonics EM31Mk2) pulled on a sledge across the ice (Haas, 2004). With GEM measurements, the distance to the ice–water interface corresponds to the ice plus snow thickness. After 2001, measurements were made with an airborne EM (AEM) system towed 12 to 20 m above the ice surface. Here, the distance to the uppermost snow surface is determined with a laser altimeter. The ice plus snow thickness is then calculated as the difference between the laser and EM derived distance (Haas et al., 2009). In 2004, AEM measurements were conducted with a helicopter operated from RV *Polarstern* (cruise ARK-XX/2) along triangular flight tracks with a side length of 40 to 80 km (Haas et al., 2008). In 2010, 2011 and 2012 AEM surveys were conducted with the *Polar 5* aircraft during the TIFAX (Thick Ice Feeding Arctic Export) campaigns operating from the Danish Station Nord in Nord-East Greenland (Haas et al., 2010). These airplane surveys allow the acquisition of hundreds of kilometers of data along straight flight lines. An overview of the flight tracks surveyed during the individual field campaigns is given in Fig. 1.

The accuracy of the EM measurements is on the order of ± 0.1 m over level sea ice (Pfaffling et al., 2007). However the maximum thickness of pressure ridges can be underestimated by as much as 50 %. The underestimation of peak pressure ridge thickness is a result of footprint smoothing, an effect that is mass-conserving for mean thickness values on kilometer scale. Thus, mean ice thickness values from AEM data

Fram Strait sea ice thickness and summer export

T. Krumpfen et al.

Title Page

Abstract

Introduction

Conclusions

References

Tables

Figures



Back

Close

Full Screen / Esc

Printer-friendly Version

Interactive Discussion



Fram Strait sea ice thickness and summer export

T. Krumpen et al.

Title Page

Abstract

Introduction

Conclusions

References

Tables

Figures



Back

Close

Full Screen / Esc

Printer-friendly Version

Interactive Discussion



are in general agreement with other sources (Lindsay and Schweiger, 2015), such as ULS, though the probability density function (pdf) may differ slightly (Mahoney et al., 2014). Still, the AEM thickness pdf enables us to determine the general thermodynamic and dynamic boundary conditions of ice formation (Thorndike et al., 1975; Maykut, 1985). The thickness pdf's for all profiles presented in this paper were calculated from histograms with a bin width of 0.1 m. The most frequently occurring ice thickness, the mode of the distribution, represents level ice thickness and is the result of winter accretion and summer ablation. Because ridge thicknesses are in general underestimated in AEM data, the mode is most representative for the ice thickness pdf. The fraction of dynamically deformed ice is represented by the length and the shape of the tail of the thickness distribution. In this study, the fraction of ice thicker than 3 m is used to give a relative estimate of the amount of deformed ice. The mean thickness is used to quantify the overall decline in sea ice thickness. Note that before calculating mean and modal thickness from the pdf's, ice thinner than 0.15 m was excluded from the analysis, as we categorize this thickness category as open water bin due to the 10 cm noise of the EM sensor. For the investigation of across and along Fram Strait thickness gradients, pdf's, mean and mode were calculated over a 25 km distance for meridional profiles (along Fram Strait) and zonal profiles (across Fram Strait).

Since per definition EM ice thickness measurements include the snow layer, interannual changes in ice thickness may not be solely related to changes in ice thickness, but also to changes in snow cover. However, even though snow thickness during EM surveys may not have been at its minimum, we believe that temperatures above freezing had certainly led to a significantly reduced snow cover or no snow cover at all (Warren et al., 1999). Hence, we assume the bias that arises from the unknown snow thickness to be negligible.

The examination of interannual changes in the sea ice cover over a certain area requires continuous and overlapping measurements. Despite shortcomings due to logistical and meteorological challenges of air- and shipborne campaigns in the Arctic, we consider our data set to be sufficiently homogenous with respect to its temporal

Fram Strait sea ice thickness and summer export

T. Krumpen et al.

Title Page

Abstract

Introduction

Conclusions

References

Tables

Figures



Back

Close

Full Screen / Esc

Printer-friendly Version

Interactive Discussion



and spatial coverage. Nevertheless, to ensure a maximum degree of consistency and to limit bias due to warm Atlantic Water (Beszczynska-Moeller et al., 2012), only flights obtained between 82 and 85° N and 13° W and 20° E were selected (compare the red shaded area in Fig. 1). A summary of the survey flights obtained during individual campaigns is presented in Table 1 together with survey dates and length of EM-profiles. In addition, the modal and mean ice thickness, as well as fraction of ice ≥ 3 m and the open water fraction are given.

2.2 Satellite data

The interpretation of EM thickness measurements requires information about the age, drift history, and source areas of the surveyed ice. Below we describe the data set that was used to determine age and drift trajectories. In addition, we present the approach to quantify ice area fluxes through Fram Strait.

2.2.1 Sea ice concentration

Sea ice concentration data used in this study are obtained from the National Snow and Ice Data Center (NSIDC). The data set was derived using measurements from the Scanning Multichannel Microwave Radiometer (SMMR) aboard the Nimbus-7 satellite, from the Special Sensor Microwave/Imager (SSM/I) on the -F8, -F11, and -F13 satellites of the Defense Meteorological Satellite Program (DMSP), and from Microwave Imager/Sounder (SSMIS) aboard DMSP-F17. Sea ice concentration was calculated based on the Bootstrap algorithm (Comiso, 2000). Data are available on a daily basis at 25 km \times 25 km spatial resolution.

2.2.2 Sea ice drift

Passive-microwave retrieved ice drift products are provided by different institutions and have been widely used in sea ice studies and for model assimilation (e.g. Miller et al., 2006; Kwok, 2009; Spreen et al., 2011; Sumata et al., 2014). In this study, two different

Fram Strait sea ice thickness and summer export

T. Krumpfen et al.

Title Page

Abstract

Introduction

Conclusions

References

Tables

Figures



Back

Close

Full Screen / Esc

Printer-friendly Version

Interactive Discussion



sets of ice drift products were used: The first data set, Polar Pathfinder Sea Ice Motion Vectors (Version 2), was chosen because of its good performance and year round availability. Below it is used to estimate transport rates out of Fram Strait, and to calculate ice drift trajectories during summer months (June–August). The product provided by the NSIDC contains daily gridded fields of sea ice motion on a 25 km Equal Area Scalable Earth grid (EASE) for the period between 1978 to 2012 (Fowler et al., 2013). The motion vectors (hereafter referred to as NSIDC) are obtained from a variety of satellite-based sensors such as the SMMR, SSM/I, AMSR-E and Advanced Very High Resolution Radiometer (AVHRR) and buoy observations from the International Arctic Buoy Program (IABP). A description of the data set and the sea ice motion retrieval algorithm can be found in Fowler et al. (2013).

In addition to NSIDC drift data, the tracking routine as described in Sect. 2.2.3 makes use of motion estimates provided by the Center for Satellite Exploitation and Research (CERSAT) at the Institut Francais de Recherche pour d'Exploitation de la Mer (IFREMER), France. Since a substantial part of Fram Strait sea ice originates from the Laptev Sea (Rigor and Colony, 1997), the calculation of drift trajectories requires a drift data set with good performance on the Siberian shelf. Following Rozman et al. (2011) and Krumpfen et al. (2013), a comparison of different drift products with high resolution satellite and in-situ drift data in the Laptev Sea have shown that the CERSAT motion data has the highest accuracy in this region. Hence, the ice drift data provided by CERSAT were used in the tracking approach, bridged with NSIDC data during summer months. The motion fields (hereafter referred to as CERSAT) are based on a combination of drift vectors estimated from scatterometer (SeaWinds/QuikSCAT and ASCAT/MetOp) and radiometer (SSM/I) data. They are available with a grid size of 62.5 km, using time intervals of 3 days for the period between September and May (1991 to present).

2.2.3 Sea ice pathways and source areas

To determine drift trajectories and source areas of sampled sea ice we tracked the surveyed ice backward over a period of four years using NSIDC and CERSAT ice drift and NSIDC ice concentration products. A specific floe is tracked backwards until: (a) the ice reaches a position next to a coastline, (b) the ice concentration at a specific location reaches a threshold value of ($\leq 15\%$) where the ice is assumed to be melted, or (c) the tracking time exceeds four years.

2.2.4 Ice age

Sea ice age information was obtained from the drift-age model of Maslanik et al. (2011). Ice age is retrieved by tracking sea ice from the formation until the melt or export using NSIDC ice concentration and drift data. The data set is available on a $25\text{ km} \times 25\text{ km}$ grid with a temporal resolution of one week for the period between January 1990 and August 2013. For more details we refer to Maslanik et al. (2011).

2.2.5 Ice area flux across Fram Strait

In Sect. 3.4 we relate recent changes observed in Fram Strait ice thickness to satellite based estimates of ice area flux. Ice area flux estimates out of Fram Strait are calculated using NSIDC motion estimates together with NSIDC ice concentration information. Flux estimates are made along a zonal gate positioned at 82° N , between 12° W and 20° E and a meridional gate that connects the eastern end of the zonal gate with Spitzbergen (80.6° N , 20° E , compare Fig. 1). The ice area flux at the meridional and zonal flux gates is the integral of the product between the V and U drifts and ice concentration. In the following, ice area flux across Fram Strait is referred to as the sum of the meridional and zonal ice fluxes. A positive (negative) sign refers to an export out of (import into) the Arctic Ocean. Transport (flux) rates are given in $\text{km}^2\text{ day}^{-1}$ or month^{-1} . After removing the seasonal cycle, trends were calculated by linear regres-

Fram Strait sea ice thickness and summer export

T. Krumpfen et al.

Title Page

Abstract

Introduction

Conclusions

References

Tables

Figures



Back

Close

Full Screen / Esc

Printer-friendly Version

Interactive Discussion



Fram Strait sea ice thickness and summer export

T. Krumpen et al.

Title Page

Abstract

Introduction

Conclusions

References

Tables

Figures



Back

Close

Full Screen / Esc

Printer-friendly Version

Interactive Discussion



the past 11 years, with a distinct reduction in ice thickness after 2004, when the mode dropped by 36 % from 2.2 m (2004) to 1.4 m (2012). Similar to observations in 2007 at the North Pole by Haas et al. (2008), the interannual variability in modal thickness can be explained to some degree by different age compositions. For instance, the higher modal thickness in 2004 is likely the consequence of predominantly older ice (compare Fig. 3). However, there is no evidence of a change in age composition of surveyed ice towards younger ice that could explain the overall decline in ice thickness. In fact, the age of surveyed ice in 2010 and 2012 does not differ much from 2001, but the modal thickness is significantly lower. Therefore, we assume that the decline in modal thickness observed in Fram Strait rather reflects the thinning of second-year and multiyear ice in the Laptev Sea (source area) and Transpolar Drift than decreasing age. The decrease in modal thickness is accompanied by a decrease in ridged ice (fraction of ice thicker than 3 m). Note that in 2001 and 2004, the fraction of deformed ice is twice as high as in 2010, 2011 or 2012. Similar to the modal ice thickness, some of the interannual variability may be related to a varying age composition, but the overall decline is independent of ice age. Hence, the reduction of the deformed ice fraction points to a reduction in the deformation history in source areas and along pathways, mainly in the Laptev Sea and along the Transpolar Drift, which is in agreement with findings of Hansen et al. (2013). The shrinking tail of the ice thickness distribution as well as the decrease in modal ice thickness is also reflected in the mean thickness. Figure 4 shows that during the past 11 years the mean thickness dropped by 16 % from 2.58 m in 2001 to 2.17 m in 2012. A slight increase in mean thickness takes place after 2010. The increase is related to an increase in the fraction of deformed ice between 2010 and 2012.

The comparison of AEM and GEM based observations may introduce an additional uncertainty and must be limited to a comparable range of the thickness distribution. Although GEM data were obtained on a daily basis at representative locations along the ship track, the ground-based thickness surveys of 2001 are limited to large floes and predominantly level ice thick enough to walk on. In addition, the footprint of ground-

5 In Sect. 2.2.3, we estimated the transit time of sea ice between 79 and 81° N to be around 80 days. If the thinning is produced by ocean heat fluxes this implies a mean ocean heat flux of 16 W m^{-2} . This is clearly within the range of observed ocean heat fluxes in the area (Sirevaag, 2009), but higher than observed Arctic Basin values in the range $2\text{--}5 \text{ W m}^{-2}$ (Fer, 2009).

10 In 2012, a second 170 km long flight in upstream direction was performed. Measurements were a continuation of the transect made in 2011 and started at 80.5° N. The ice cover was again rather homogenous with a few leads. According to Fig. 2 ice was formed in the western Laptev Sea and transported via the Transpolar Drift towards Fram Strait. The absence of a gradient in modal thickness indicates that enhanced bottom melt due to presence of AW branches is limited to areas south of $\approx 80^\circ \text{ N}$. Marnela et al. (2013) found the recirculation to be weaker close to 80° N than close to 78° N, with strongest effects at 79° N.

15 The ice thickness gradient across Fram Strait was investigated during two flights in 2010 (22 August) and 2012 (21 July). The long operating distance of *Polar 5* enabled us to obtain the first continuous profiles over closed ice pack north of 81° N. The across strait ice thickness profile is presented in Fig. 6b. Both transects show a negative trend in modal (0.02 m and $0.04 \text{ m degree}^{-1}$ longitude) and mean (0.03 m and $0.11 \text{ m degree}^{-1}$ longitude) ice thickness from West to East. The gradient in mean thickness is thereby more pronounced than the gradient in modal thickness. For sea ice at this latitude or higher, one can assume the impact of warm water on the ice cover to be small. This assumption is supported by the absence of a gradient in modal ice thickness for sea ice upstream of 80.5° N and hydrographic observations of Marnela et al. (2013) discussed above. Hence, we assume the observed gradient to be mainly associated with differences in age and deformation of ice provided by the Transpolar Drift system. A comparison to Fig. 2 reveals that the ice that enters Fram Strait west of the prime meridian is indeed older and therefore most likely thicker than ice that enters through the eastern section. Note that the good agreement between the length of path-

Fram Strait sea ice thickness and summer export

T. Krumpfen et al.

Title Page

Abstract

Introduction

Conclusions

References

Tables

Figures



Back

Close

Full Screen / Esc

Printer-friendly Version

Interactive Discussion



ways and observed thickness gives us confidence in the performance of the tracking approach.

Earlier quantifications of across strait gradients were made by Hansen et al. (2013) and Renner et al. (2014) approximately 300 km further south at 79° N. Their estimates are based on interpolations between single point upward looking sonar measurements and on merged EM profiles obtained during different days. For this position, the authors reported a decline in across strait modal thickness of -0.1 to -0.3 m degree⁻¹ longitude (Renner et al., 2014) and -0.23 m degree⁻¹ longitude (Hansen et al., 2013). It stands to reason that the stronger gradient observed at 79° N can be explained by an increasing strength of the AW recirculation in downstream direction.

3.4 Summer sea ice area and volume fluxes

To quantify whether coupled sea ice ocean models are capable of reproducing Fram Strait sea ice volume fluxes correctly, validation data are required. Using satellite data, the volume flux in Fram Strait can be described as the product of southward directed sea ice motion, concentration and mean thickness. Information on ice drift and concentration is available on a year round basis. However, the availability of satellite based thickness data from ICESat or CryoSat-2 are restricted to winter months, which is why ice volume flux estimates for summer periods are scarce. In the following, we will therefore use the presented AEM measurements together with satellite based area flux estimates to calculate volume outflows for the periods when thickness surveys were made.

Because of its year round availability, ice area flux out of Fram Strait is calculated using NSIDC motion estimates together with NSIDC ice concentration information. Figure 7 shows the monthly ice area export across Fram Strait from 1980–2012 (orange line). Note that the area flux is the sum of meridional and zonal components, with a positive sign referring to ice export, and a negative sign indicating ice import into the Arctic (see Sect. 2.2.5). The average monthly ice area flux amounts to 46×10^3 km² with a standard deviation of 38×10^3 km². The monthly ice export shows a pronounced

Fram Strait sea ice thickness and summer export

T. Krumpen et al.

Title Page

Abstract

Introduction

Conclusions

References

Tables

Figures



Back

Close

Full Screen / Esc

Printer-friendly Version

Interactive Discussion



Fram Strait sea ice thickness and summer export

T. Krumpen et al.

Title Page

Abstract

Introduction

Conclusions

References

Tables

Figures



Back

Close

Full Screen / Esc

Printer-friendly Version

Interactive Discussion



seasonal cycle with lowest fluxes in July and August and highest export rates between December and March. During summer, flux rates are significantly lower and can become even negative, such that ice is being imported from southern Fram Strait. The pronounced seasonal cycle and much of the interannual variability of ice area export are associated with changes in SLP gradients across the gate, because gradients are generally lower during summer months and higher during winter. In addition, sea ice concentration in Fram Strait is lower during summer months, which leads to reduced export rates between July and September. Overall we find a positive trend in monthly Fram Strait area flux of $10.9 \times 10^3 \text{ km}^2 \text{ decade}^{-1}$. The trend is significant at the 99 % confidence level. Following Smedsrud et al. (2011) the increase in ice export is the consequence of a positive trend in the local pressure gradient, related to intensification of cyclones over the Nordic Seas. According to that study the sea ice area export has increased about 25 % larger since 1960s. The increase in ice export occurred mostly during winter and is directly connected to higher southward ice drift velocities, due to stronger geostrophic winds.

The area export for July, August and September accounts for only 6.2 % of the annual fluxes. The months with the lowest net contributions are July and August (1.4 %). Ice area export rates for both months are shown in Fig. 8 (blue and orange lines). The net sea ice export during July and August is positive, but estimates show considerable interannual variability with the highest rates occurring in August of 1994, 2006 and 2010 and lowest in 1981 and 1998. The average August ice area flux amounts to $4.3 \times 10^3 \text{ km}^2$ with a standard deviation (SE) of $19 \times 10^3 \text{ km}^2$. The average July ice flux is a bit lower ($3.8 \times 10^3 \text{ km}^2 \pm 13 \times 10^3 \text{ km}^2$). Note that there is a positive trend in the August and July ice export of 5.5×10^3 and $2.3 \times 10^3 \text{ km}^2 \text{ decade}^{-1}$, respectively. The trend is however not statistically significant.

The associated volume fluxes for the years where GEM/AEM measurements are available is calculated as the product of area flux and mean GEM/AEM thickness (Fig. 8). Note that for 2012, where AEM measurements were made one month earlier, area transport rates for July (blue line) were used. Given the low area export in July

and August, the volume transport is low, too. For the investigated months, the average volume export amounts to 17.77 km^3 ($\pm 34.45 \text{ km}^3$) with highest rates in August 2010 (64.83 km^3) and lowest in August 2001 (-15.97 km^3).

The reliability of volume flux depends as well upon the accuracy of sea ice motion information in summer as on the available thickness information. Following Sumata et al. (2014), ice motion information taken from passive microwave data suffer from a general underestimation of drift during summer months and a generally reduced accuracy in the narrow Fram Strait. Due to the lack of sea ice motion observations from drifting buoys, we compare our results with area flux estimates from Kloster and Sandven (2011) and Smedsrud et al. (2011) (Fig. 7, red and grey line). Area flux calculations of Kloster and Sandven (2011) are based on ice concentration data and manually derived ice motion information from ENVISAT SAR images. SAR WideSwath image pairs were captured three days apart with uninterrupted year-round coverage from February 2004 to December 2011. Estimates were made across 79° N , 15° W and 79° N , 5° E . Note that at 79° N Fram Strait is relatively narrow and therefore only a limited number of images are needed to cover the entire passage. According to the authors, the monthly mean export uncertainties amount to 5%. Smedsrud et al. (2011) used the pressure difference (NCEP/NCAR reanalysis data) between 79° N , 25° W and 79° N , 5° E together with SAR based flux estimates of Kloster and Sandven (2011) to estimate the linear regression between geostrophic winds, sea ice drift speed and ice area export. The linear relationship was then used to reconstruct ice area export based on pressure differences for the period between 1957 and 2010.

A direct comparison of our area flux estimates with the findings of Smedsrud et al. (2011) and Kloster and Sandven (2011) is difficult, because area flux estimates are based on different methods and were made at different latitude gates. Thus, we cannot quantify an absolute uncertainty associated with the volume estimates above. However, a comparison of our findings with area export estimates of others reveals that the trend in NSIDC export rates is much higher ($37.6 \text{ \% decade}^{-1}$ for the period 1980–2012) than the trend found by Kloster and Sandven (2011) ($22.2 \text{ \% decade}^{-1}$ for the

Fram Strait sea ice thickness and summer export

T. Krumpfen et al.

Title Page

Abstract

Introduction

Conclusions

References

Tables

Figures



Back

Close

Full Screen / Esc

Printer-friendly Version

Interactive Discussion



period 2004–2011, compare Fig. 7) or the trend reported by Smedsrud et al. (2011) ($4.7\% \text{ decade}^{-1}$ for the period 1980–2010). A discussion on causes of differences in observed trends is beyond the scope of this manuscript. However, it is likely that large differences are at least partially related to unrealistically low NSIDC-based sea ice motion estimates before 1995. Nevertheless, despite large differences in observed trends the concordance between our findings and estimates of Kloster and Sandven (2011) and Smedsrud et al. (2011) gives us confidence in our results. The agreement in seasonal variability indicates that there is a relative consistency between area fluxes: The correlation coefficient (r) between NSIDC based estimates and computations of Smedsrud et al. (2011) is 0.79 and between NSIDC area flux and SAR-based estimates 0.80. The agreement between SAR-, and SLP-based export rates are of the same order ($r = 0.82$). A comparison of absolute fluxes for the periods where NSIDC, NCEP/NCAR reanalysis data and SAR-based estimates are available (2004–2010) shows that our estimates are approximately 18 and 20 % lower than estimates of Smedsrud et al. (2011) and Kloster and Sandven (2011). If the intercomparison is limited to summer months only (July–September), NSIDC based export rates are within the range of SAR-based estimates ($27 \times 10^3 \text{ km}^2$ vs. $28 \times 10^3 \text{ km}^2$), whereas computations based on pressure differences are higher ($53 \times 10^3 \text{ km}^2$).

4 Conclusions

We present an extensive data set of ground-based and airborne electromagnetic (EM) ice thickness measurements covering Fram Strait and the southern part of the Transpolar Drift in summer between 2001 and 2012. The data set adds to existing ice thickness information, with the addition of long transects that can only be obtained by fixed-wing aircrafts.

An investigation of pathways and source areas of surveyed sea ice shows that the largest fraction of ice has been formed in the Laptev Sea. The average age of ice covered by EM measurements is between 2.1 and 3.3 years. Keeping limitations of the

Fram Strait sea ice thickness and summer export

T. Krumpen et al.

Title Page

Abstract

Introduction

Conclusions

References

Tables

Figures



Back

Close

Full Screen / Esc

Printer-friendly Version

Interactive Discussion



Fram Strait sea ice thickness and summer export

T. Krumpen et al.

Title Page

Abstract

Introduction

Conclusions

References

Tables

Figures



Back

Close

Full Screen / Esc

Printer-friendly Version

Interactive Discussion



rather short and irregular spaced time series in mind, the EM data provide evidence of a changing Fram Strait sea ice cover. As seen also in other, independent datasets, the observed decrease in modal thickness between 2001 and 2012 likely reflects a thinning of second-year and multiyear ice cover leaving the Arctic Basin through Fram Strait.

The decrease in modal thickness is accompanied by a decrease in mean thickness and fraction of ice thicker than 3 m.

The thinning effect of atmospheric and oceanographic processes on southward moving sea ice was investigated during two ice thickness surveys performed in downstream direction. A decrease in modal thickness of $0.19 \text{ m degree}^{-1}$ latitude south of 81° N is likely associated with the presence of recirculated warm Atlantic water, leading to enhanced bottom melt. Further north, the impact of warm water advection on the ice cover is negligible. Here, variability in ice thickness is more likely related to differences in age and deformation of ice.

Together with satellite based area flux estimates, we used our thickness measurements to calculate volume fluxes during summer months. Ice area flux estimates are performed using satellite based ice concentration and drift data. In agreement with Smedsrud et al. (2011) we find a significant positive trend in monthly Fram Strait area flux. The summer (July and August) ice export is low compared to the annual values. For the investigated months, the average volume export amounts to 17.77 km^3 ($\pm 34.45 \text{ km}^3$) with highest rates in August 2010 (64.83 km^3) and lowest in August 2001 (-15.97 km^3). Naturally, the volume flux estimates are limited to the period when airborne thickness surveys are available. Nevertheless, we could show that the combination of satellite data and airborne observations can be used to determine volume fluxes through Fram Strait and as such, be used to bridge the lack of satellite based sea ice thickness information in summer. Therefore, airborne thickness surveys in Fram Strait should be continued and extended in the future.

Acknowledgements. We thank the crew of the research aircraft *Polar-5*, the helicopter crew of RV *Polarstern*, the crew of Station Nord in Greenland, and Manuel Sellmann and Martin Gehrman (AWI) for their great logistical support and helping hands during campaigns. We

Fram Strait sea ice thickness and summer export

T. Krumpen et al.

Title Page

Abstract

Introduction

Conclusions

References

Tables

Figures



Back

Close

Full Screen / Esc

Printer-friendly Version

Interactive Discussion



- Haas, C., Lobach, J., Hendricks, S., Rabenstein, L., and Pfaffling, A.: Helicopter-borne measurements of sea ice thickness, using a small and lightweight, digital EM system, *J. Appl. Geophys.*, 67, 234–241, 2009. 5175
- Haas, C., Hendricks, S., Eicken, H., and Herber, A.: Synoptic airborne thickness surveys reveal state of Arctic sea ice cover, *Geophys. Res. Lett.*, 37, L09501, doi:10.1029/2010GL042652, 2010. 5175, 5194
- Hansen, E., Gerland, S., Granskog, M. A., Pavlova, O., Renner, A. H., Haapala, J., Loynning, T. B., and Tschudi, M.: Thinning of Arctic sea ice observed in Fram Strait: 1990–2011, *J. Geophys. Res.*, 118, 5202–5221, doi:10.1002/jgrc.20393, 2013. 5173, 5174, 5181, 5182, 5185, 5199
- Kloster, K. and Sandven, S.: Ice Motion and Ice Area Flux in Fram Strait at 79° N Using ASAR and Passive Microwave for February 2004–July 2010, Tech. report 322, Nansen Environmental and Remote Sensing Centre, Bergen, Norway, 2011. 5187, 5188, 5201
- Krumpen, T., Janout, M., Hodges, K. I., Gerdes, R., Girard-Ardhuin, F., Hölemann, J. A., and Willmes, S.: Variability and trends in Laptev Sea ice outflow between 1992–2011, *The Cryosphere*, 7, 349–363, doi:10.5194/tc-7-349-2013, 2013. 5178
- Kwok, R.: Outflow of Arctic Ocean Sea Ice into the Greenland and Barents Seas: 1979–2007, *J. Climate*, 22, 2438–2457, doi:10.1175/2008JCLI2819.1, 2009. 5174, 5177
- Kwok, R., Spreen, G., and Pang, S.: Arctic sea ice circulation and drift speed: decadal trends and ocean currents, *J. Geophys. Res.*, 118, 2408–2425, 2013. 5174
- Lindsay, R. and Schweiger, A.: Arctic sea ice thickness loss determined using subsurface, aircraft, and satellite observations, *The Cryosphere*, 9, 269–283, doi:10.5194/tc-9-269-2015, 2015. 5173, 5176
- Mahoney, A., Eicken, H., Fukamachi, Y., Ohshima, H., Shimizu, D., Kambhamettu, C., Hendricks, S., and Jones, J.: Taking a look at both sides of the ice: comparison of ice thickness and drift speed as observed from moored, airborne and shore-based instruments near Barrow, Alaska, *Ann. Glaciol.*, 69, 69A565, 2014. 5176
- Marnela, M., Rudels, B., Houssais, M.-N., Beszczynska-Möller, A., and Eriksson, P. B.: Recirculation in the Fram Strait and transports of water in and north of the Fram Strait derived from CTD data, *Ocean Sci.*, 9, 499–519, doi:10.5194/os-9-499-2013, 2013. 5184
- Martin, T., Steele, M., and Zhang, J.: Seasonality and long-term trend of Arctic Ocean surface stress in a model, *J. Geophys. Res.*, 119, 1723–1738, doi:10.1002/2013JC009425, 2014. 5173

Fram Strait sea ice thickness and summer export

T. Krumpfen et al.

Title Page

Abstract

Introduction

Conclusions

References

Tables

Figures



Back

Close

Full Screen / Esc

Printer-friendly Version

Interactive Discussion



- Maslanik, J. A., Stroeve, J., Fowler, C., and Emery, W.: Distribution and trends in Arctic sea ice age through spring 2011, *Geophys. Res. Lett.*, 38, L13502, doi:10.1029/2011GL047735, 2011. 5179
- 5 Maykut, G. A.: The Surface Heat and Mass Balance, the Geophysics of Sea Ice, Martinus Nijhoff Publ., Dordrecht, 1985. 5176
- Meier, W. N., Hovelsrud, G. K., van Oort, B. E., Key, J. R., Kovacs, K. M., Michel, C., Haas, C., Granskog, M. A., Gerland, S., Perovich, D. K., Makshtas, A., and Reist, J. D.: Arctic sea ice in transformation: a review of recent observed changes and impacts on biology and human activity, *Rev. Geophys.*, 52, 185–217, doi:10.1002/2013RG000431, 2014. 5172
- 10 Miller, P. A., Laxon, S. W., Feltham, D. L., and Gresswell, J.: Optimization of a sea ice model using Basinwide observations of arctic sea ice thickness, extent, and velocity, *J. Climate*, 19, 1089–1108, doi:10.1175/JCLI3648.1, 2006. 5177
- Pfaffling, A., Haas, C., and Reid, J. E.: A direct helicopter EM sea ice thickness inversion, assessed with synthetic and field data, *Geophysics*, 72, F127–F137, 2007. 5175
- 15 Rabenstein, L., Hendricks, S., Martin, T., Pfaffhuber, A., and Haas, C.: Thickness and surface properties of different sea ice regimes within the Arctic Trans Polar Drift: data from summers 2001, 2004 and 2007, *J. Geophys. Res.*, 115, C12059, doi:10.1029/2009JC005846, 2010. 5174
- Rampal, P., Weiss, J., and Marsan, D.: Positive trend in the mean speed and deformation rate of Arctic sea ice, 1979–2007, *J. Geophys. Res.*, 114, C05013, doi:10.1029/2008JC005066, 2009. 5173
- 20 Renner, A. H., Gerland, S., Haas, C., Spreen, G., Beckers, J. F., Hansen, E., Nicolaus, M., and Goodwin, H.: Evidence of Arctic sea ice thinning from direct observation, *Geophys. Res. Lett.*, 41, 5029–5036, doi:10.1002/2014GL060369, 2014. 5173, 5174, 5182, 5183, 5185, 5199
- 25 Rigor, I. G. and Colony, R. L.: Sea-ice production and transport of pollutants in the Laptev Sea, 1997–1993, *Sci. Total Environ.*, 202, 89–110, doi:10.1016/S0048-9697(97)00107-1, 1997. 5178
- Rozman, P., Hoelemann, J., Krumpfen, T., Gerdes, R., Koeberle, C., Lavergne, T., and Adams, S.: Validating satellite derived and modelled sea-ice drift in the Laptev Sea with in situ measurements from the winter of 2007/08, *Polar Res.*, 30, 67218, doi:10.3402/polar.v30i0.7218, 2011. 5178
- 30

Fram Strait sea ice thickness and summer export

T. Krumpen et al.

Title Page

Abstract

Introduction

Conclusions

References

Tables

Figures

◀

▶

◀

▶

Back

Close

Full Screen / Esc

Printer-friendly Version

Interactive Discussion



- Sirevaag, A.: Turbulent exchange coefficients for the ice/ocean interface in case of rapid melting, *Geophys. Res. Lett.*, 36, L0460, doi:10.1029/2008GL036587, 2009. 5184
- Smedsrud, L. H., Sirevaag, A., Kloster, K., Sorteberg, A., and Sandven, S.: Recent wind driven high sea ice area export in the Fram Strait contributes to Arctic sea ice decline, *The Cryosphere*, 5, 821–829, doi:10.5194/tc-5-821-2011, 2011. 5174, 5186, 5187, 5188, 5189, 5201
- Spreen, G., Kern, S., Stammer, D., and Hansen, E.: Fram Strait sea ice volume export estimated between 2003 and 2008 from satellite data, *Geophys. Res. Lett.*, 36, L19502, doi:10.1029/2009GL039591, 2009. 5174
- Spreen, G., Kwok, R., and Menemenlis, D.: Trends in Arctic sea ice drift and tole of wind forcing: 1992–2009, *Geophys. Res. Lett.*, 38, 1–14, doi:10.1029/2011GL048970, 2011. 5173, 5177
- Sumata, H., Lavergne, T., Girard-Arduin, F., Kimura, N., Tschudi, M., F., K., Karcher, M., and Gerdes, R.: An intercomparison of Arctic ice drift products to deduce uncertainty estimates, *J. Geophys. Res.*, 119, 4887–4921, doi:10.1002/2013JC009724, 2014. 5177, 5187
- Thorndike, A. S., Rothrock, D. A., Maykut, G. A., and Colony, R.: The thickness distribution of sea ice, *J. Geophys. Res.*, 80, 4501–4513, 1975. 5176
- Vavrus, S. J., Holland, M. M., Jahn, A., Bailey, D., and Blazey, B. A.: Twenty-first-century Arctic climate change in CCSM4, *J. Climate*, 25, 2696–2710, doi:10.1175/JCLI-D-11-00220.1, 2012. 5173
- Warren, S. G., Rigor, I. G., Untersteiner, N., F., R. V., Bryzgin, N. N., Aleksandrov, Y. I., and Colony, R.: Snow depth on Arctic sea ice, *J. Climate*, 12, 1814–1829, 1999. 5176

Fram Strait sea ice thickness and summer export

T. Krumpen et al.

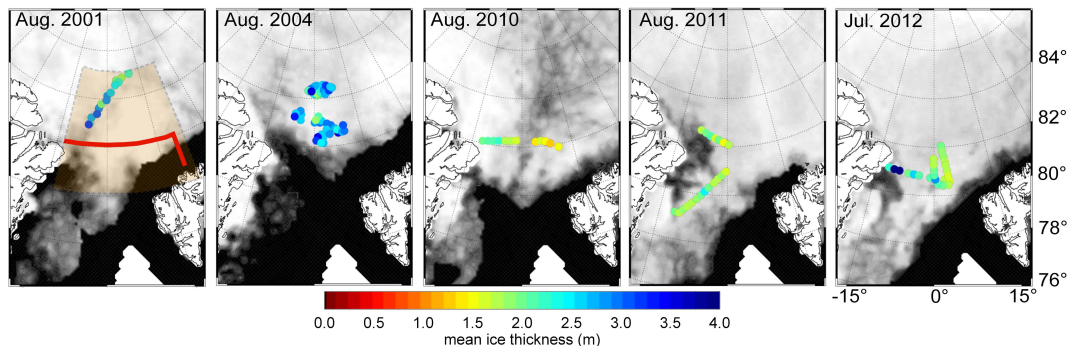


Figure 1. Overview of all EM ice thickness measurements obtained in the Fram Strait region during two cruises with the German ice-breaker RV *Polarstern* (August 2001 and 2004) and three surveys with the research aircraft *Polar-5* (August 2010 and 2011, July 2012). The color coding of the EM profiles corresponds to the mean ice thickness of 10 km sections. The light red shaded area marks the area of interest with the data acquisitions used in this analysis. Ice concentration at first flight of each campaign, is plotted in the background. The thick red line in the left panel indicates the meridional and zonal gates through which satellite derived ice area fluxes were calculated.

[Title Page](#)[Abstract](#)[Introduction](#)[Conclusions](#)[References](#)[Tables](#)[Figures](#)[◀](#)[▶](#)[◀](#)[▶](#)[Back](#)[Close](#)[Full Screen / Esc](#)[Printer-friendly Version](#)[Interactive Discussion](#)

Fram Strait sea ice thickness and summer export

T. Krumpen et al.

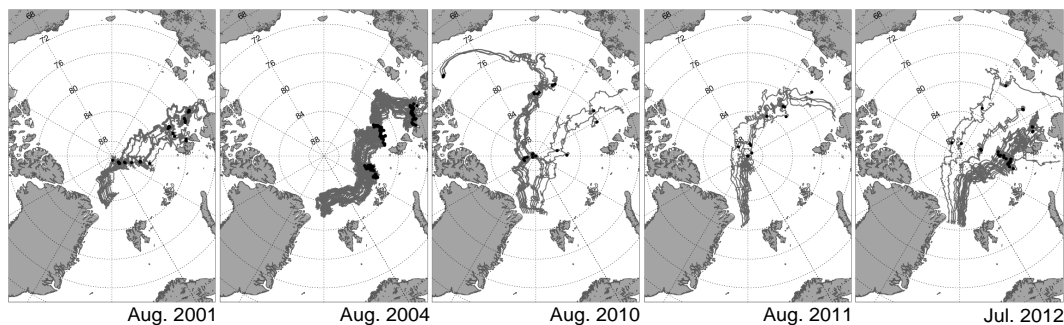


Figure 2. Backtracking of sampled sea ice using a combination of ice drift and concentration information. The start points of the trajectories (grey lines) are equivalent to the positions where EM measurements were obtained during the individual years. The black dots correspond to the position of particles on 21 September, when first-year ice becomes second-year ice, and second-year ice becomes multiyear ice.

[Title Page](#)[Abstract](#)[Introduction](#)[Conclusions](#)[References](#)[Tables](#)[Figures](#)[Back](#)[Close](#)[Full Screen / Esc](#)[Printer-friendly Version](#)[Interactive Discussion](#)

Fram Strait sea ice thickness and summer export

T. Krumpen et al.

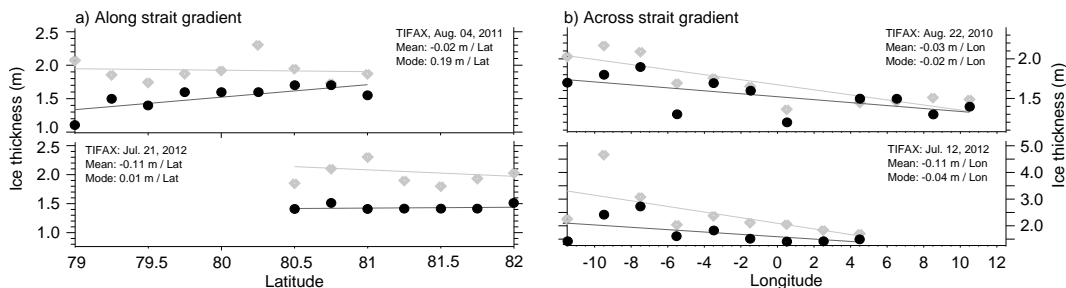


Figure 6. Across and along strait thickness gradient: **(a)** shows the along strait gradient in ice thickness (m) for flights made in August 2011 and 2012 between 10° W and 0° E. The across strait gradient as obtained from two flights in 2010 (at 81° N) and 2012 (at 82° N) is given in **(b)**. Grey rectangles correspond to the mean thickness, whereas black circles indicate modal thickness. The corresponding trend lines are plotted on top.

Fram Strait sea ice thickness and summer export

T. Krumpen et al.

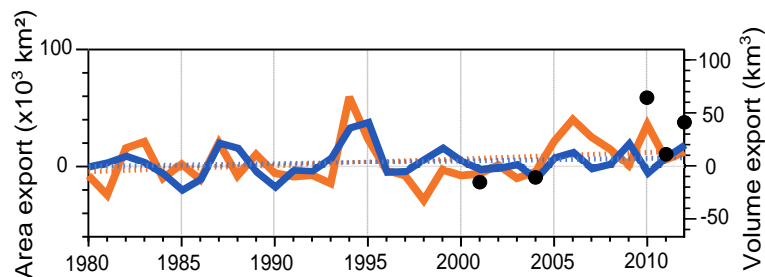


Figure 8. July (blue line) and August (orange line) ice area export across Fram Strait (given in $\times 10^3 \text{ km}^2$) calculated from NSIDC drift and concentration data. The associated volume flux for the years where AEM measurements are available is calculated as the product of NSIDC area flux estimates (August) and AEM mean thickness (black dots, given in km^3 , right axis). Note that for 2012, where AEM measurements were made one month earlier, area transport rates for July were used to number the corresponding volume flux.

Title Page

Abstract

Introduction

Conclusions

References

Tables

Figures

◀

▶

◀

▶

Back

Close

Full Screen / Esc

Printer-friendly Version

Interactive Discussion

